Available online at www.sciencedirect.com
SCIENCE DIRECT®
Journal of Nuclear Materials 335 (2004) 280–285
journal of nuclear materials
www.elsevier.com/locate/jnucmat

Turbulent heavy liquid metal heat transfer along a heated rod in an annular cavity

C.-H. Lefhalm, N.-I. Tak, H. Piecha, R. Stieglitz *

Institute for Nuclear and Energy Technologies (IKET), KALLA-Team, Forschungszentrum Karlsruhe, P.O. Box 3640, D-76021 Karlsruhe, Germany

Abstract

Heavy liquid metals (HLM) are considered as coolant and spallation material in accelerator driven systems (ADS), because of their good molecular heat conductivity. This property leads to a separation of the spatial extension of thermal and viscous boundary layers. Commercially available computational fluid dynamic codes (CFD) assume an analogy of momentum and energy transfer, which is problematic for liquid metals flow. Therefore, benchmark experiments are required, in order to validate codes or modify existing models used therein. Within this article an experimental and numerical study of a thermally developing turbulent lead bismuth (PbBi) flow along a uniformly heated rod in a circular tube is presented. Local temperatures and velocity distributions are measured using thermocouples and Pitot tubes. The data are compared to simulation results computed with the CFX code package. The measured velocity profiles coincide nearly perfect with the simulation results. However, discrepancies up to 7% between the measured and computed temperatures appear. A minor part of the deviations can be explained by the imperfect experimental set-up. But, the measured shape of the thermal boundary is different to the calculated one, indicating the inadequateness of the presently used models describing the turbulent heat transport within the thermal boundary layer.

1. Introduction

Liquid metals are often considered as coolant for an efficient heat removal of thermally high loaded surfaces because of their high thermal molecular conductivity. Their high specific heat conductivity expressed by a low molecular Prandtl numbers *Pr* yields in numerical simulations to many problems, since the viscous and the thermal length scales separate.

In order to determine the structure temperatures in a spallation target with sufficient accuracy, adequate turbulence models are required to predict the temperature field in the cooling fluid. Standard models, which are used in commercial codes, are not suitable for the simulation of convective heat transfer in heavy liquid metals with important buoyancy effects. The models using a turbulent Prandtl number to describe the turbulent heat transport assume the Reynolds analogy between the convective transport of momentum and heat. This assumption is not valid for liquid metals because the momentum field is mainly turbulence dominated and thus owns only thin viscous wall layers, whereas the temperature field is less turbulence dominated and has thick

* Corresponding author. Tel./fax: +49 7247 82 3462.
E-mail address: robert.stieglitz@iket.fzk.de (R. Stieglitz).

0022-3115/$ - see front matter © 2004 Elsevier B.V. All rights reserved.
doi:10.1016/j.jnucmat.2004.07.028

wall adjacent boundary layers governed by molecular conduction.

Therefore, improved turbulent heat transfer modelling for liquid metals requires more sophisticated methods. Additional transport equations have to be used which characterize the statistics of the temperature fluctuations which have a time scale completely different from the velocity fluctuations. In this context the normally used constants of the k–ε turbulence model or other turbulence models (like Reynolds stress model, k–ω model) which are used in commercially available code packages lead to considerable differences to the experimental values. The deviations between simulations and experiments usually increase in the weakly turbulent regime, where buoyancy plays a non-negligible role. Here, only strongly modified models like the TMBF turbulence model [1], which consists of a combination of a low Reynolds number k–ε model and a second order 5-equation heat flux model, lead to satisfactory results. Certain model extensions for liquid metal flows were developed and implemented in the TMBF based on the analysis of data from direct numerical turbulence simulations as realized in [2]. Also strong deviations between numerical predictions and experimental results have been found in thermally developing flows, see [3,4], where the heat exchange through the boundary layer plays a significant role.

Within this article we compare numerical and computational results for a hydraulically fully developed turbulent lead bismuth flow facing a sharp edged heated rod in a circular duct. In this configuration a high degree of instrumentation is realized, in order to serve as a data basis for a numerical benchmark. In fact the experiment described here was part of the ASCHLIM benchmark (assessment for computational codes in heavy liquid metal flows) of the EU [5] to qualify commercially available CFD codes for HLM applications.

2. Experimental set-up

In the heated rod experiment a turbulent PbBi flow is facing a sharp edged heated rod as depicted in Fig. 1(c). In order to ensure a hydraulically fully developed flow a flow straightener is installed 2400 mm upstream the fluid facing rod tip (Fig. 1(a)). The flow straightener has in its entrance four wings in order to break the secondary flow from the 90°-bend. Afterwards a Venturi-tube is located and it finishes with a fine grid for flow equalization. Photographs of the in- and outlet configuration are shown in Fig. 1(a) and (c). The heated rod experiment is installed within the THESYS loop of the Karlsruhe lead laboratory KALLA laboratory, which is semi-technically sketched in Fig. 1(b).

The circular main duct has an inner diameter of 60 mm and a wall thickness of 6.02 mm. To minimize the heat losses to the environment a 150 mm thick thermal insulation with a heat conductivity of 0.043 W/mK has been used. The heated rod is positioned concentrically within the main tube. The heated length l of the rod is $l = 228$ mm, its outer diameter is $d = 8.2$ mm and it can be traversed axially in z-direction by 300 mm. The non-heated cylindrical part of the rod facing the flow is 28 mm long and the tip has a length of 24.6 mm. All upstream located non-heated parts of the rod consist of stainless steel owing a heat conductivity of 14.5 W/mK. The helically fabricated DC heater located inside the rod is covered by a well thermally conducting layer and finally enclosed in a 0.5 mm thick stainless steel tube. The helix is directly DC current heated and provides a maximum heat flux of 8 kW. After the heated part the rod continues as a steel tube with a wall thickness of 2 mm housing inside the electric power supply cables. A detailed scheme of the heated rod with the below used coordinate system is depicted in Fig. 2(a).

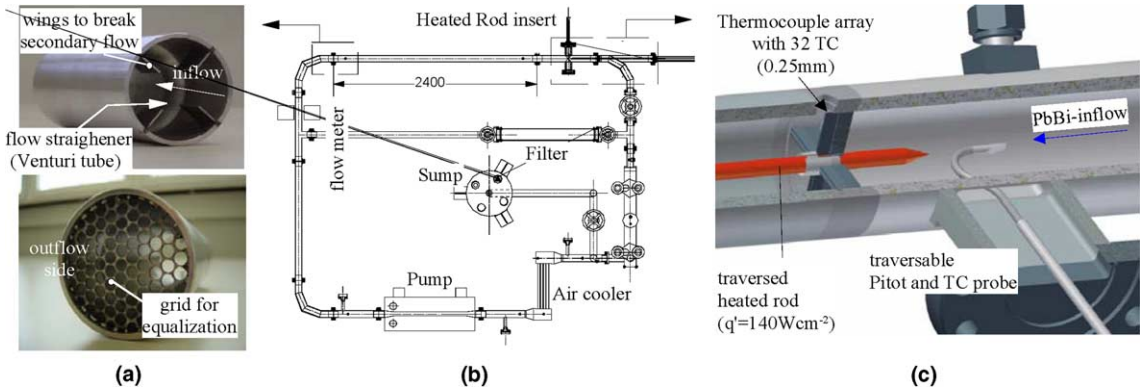

Fig. 1. Installation of the heated rod experiment in the THESYS loop of KALLA (b), with the used flow straightener (a) and the test part in the loop (c).

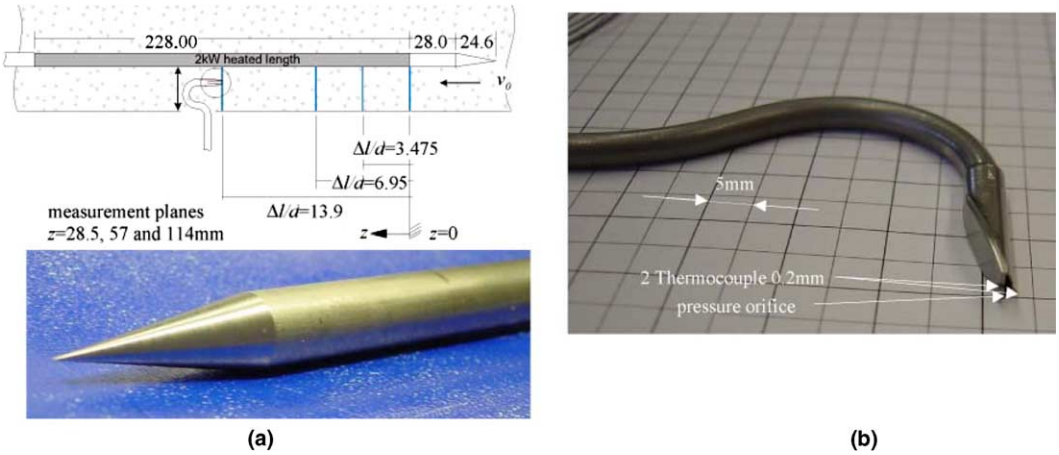

Fig. 2. (a) Geometry of the heated rod; introduction of used coordinate system; photograph of the heating rod tip; (b) photograph of the combined Pitot tube with the 2 TC's.

The temperature measurements within the liquid are performed simultaneously with 32 thermocouples (outer diameter 0.25) arranged on four wings at several discrete positions z/d. The smallest distance between thermocouple and wall is 0.1 mm. In order to ensure that the TC's measure the fluid temperature, they are fixed in such a way in the wing that the sensing tip is 1 mm from the wing facing the flow. The resolution of the calibrated thermocouples is ±0.05 K. The mean velocity is recorded using a Pitot tube with two simultaneously attached TC's, see Fig. 2(b). The piping of the Pitot tube is connected to a pressure transducer allowing the measurement of surface integrated local velocities with an accuracy of ±5 mm/s.

The flow rate in the test section is continuously controlled with an electro-magnetic frequency flow meter (EMFM) as well as the pump power. During operation the flow rate V varies in the range of $\Delta V/V$ of less than ±0.3%; a similar accuracy has the EMFM as well as the heater power supply. The temperature during operation can be kept with a stability of ±0.1 K to ensure constant inlet conditions. In order to determine the temperature losses through the environment in the region of the test module a set of thermocouples is installed within the liquid metal, at the outside of the tubing and at the outside of the thermal insulation of the test rig.

For the measurements a reference temperature of 300 °C has been chosen. This corresponds to a Prandtl number of the fluid of $Pr = 0.022$. The heating power of the rod was fixed to 2 kW, which corresponds to $q'' = 34.051$ W/cm^2. The mean fluid velocity v_0 has been varied from $6.325 \leqslant v_0$ (cm/s) $\leqslant 27.5$ equivalent to a Reynolds number range of $2.3 \times 10^4 \leqslant Re \leqslant 10^5$. For this set-up the heat losses throughout the whole test module amount to less than 147 W/m^2.

3. Numerical simulation

Numerical simulations for the heat rod experiment have been performed using the CFX code [6]. Here, the flow was considered as steady ($\partial/\partial t = 0$), incompressible (ρ = constant) and highly turbulent. Further the following simplifications have been assumed:

(a) properties of lead–bismuth and structure materials are constant and from [7];
(b) inlet profiles of velocity, temperature, and turbulence quantities are uniform;
(c) constant heat flux is generated from the heated section of the rod;
(d) effects of two side chambers for experimental measurements are neglected.

The calculations were done with 3D structured grid and special attention has been paid to keep the first grid point from the wall in the range of $30 \leqslant y^+ \leqslant 50$. Here, y^+ is defined as the dimensionless distance from the wall. The total number of meshes used is 3.32×10^4. For the flow calculation in the main flow the standard k–ε model has been used. Close to the wall the model is switched to the low Reynolds number k–ω model. Also a constant turbulent Prandtl number $Pr_t = 0.9$ has been set. Within the simulation a first order hybrid differencing scheme has been used for the advection terms. In order to examine the effect of buoyancy a second 3D calculation was performed. The developing length of the flow has been enlarged to the full one. Except for the entrance length, the other geometrical dimensions have been kept unchanged and also the thermal insulation has been taken into account using a constant temperature at the outer part of the insulation.

4. Experimental results and discussion

In Fig. 3(a) the measured velocity and temperature distribution is shown as a function of the radius r for a Reynolds number of $Re = 10^5$ in the isothermal case. The velocity profile coincides with the numerical calculations with an accuracy better than 2%. Thus the flow can be considered to be hydraulically fully developed before entering the rod region. The same holds for the temperature distribution, which exhibits almost no radial gradients. Hence, in the numerical simulation adiabatic boundary conditions ($\partial q/\partial n = 0$) are justified.

In Fig. 3(b) the measured velocity and temperature rise (ΔT) distributions are shown as a function of the radius r at several discrete positions z/d. Although the closest velocity measurement position to the rod is 2 mm away from it, a part of the developing momentum boundary layer could be captured by the Pitot probe. The momentum boundary hardly increases in its radial extension as the flow proceeds downstream. Also the mean velocity profile remains to the first order unchanged with growing z/d. This is not surprising since the displacement thickness of the boundary layer δ_{dt} scales as $\delta_{dt} \sim Re^{-1/2}$ according to [8,9], where the Reynolds number is built with the length of the object the fluid is passing through. Due to the high Re the displacement thickness hardly increases and in the direction to the outer duct wall the velocity decreases monotonically for all z/d reaching its lowest value at $r = 0$. The mean velocity value of u_z is not zero there because the Pitot can measure in a cavity at $z = 0$, where an eddy velocity remains at that position.

The corresponding temperature graph shows that the thermal boundary layer grows continuously with increasing z/d. For $z/d > 13.57$ no further radial extension of the thermal boundary layers is observed, indicating a secondary flow superimposed to the main one. This may be caused by a starting non-concentricity of the rod within the tube, which is supported by non-symmetric temperature readings at the wall near thermocouples.

By throttling the valve the flow rate can be regulated, which allows to measure different Reynolds numbers in the range $2.3 \times 10^4 \leqslant Re \leqslant 10^5$. The measured velocity profiles as a function of the radius are depicted in Fig. 4(a). The figure shows that the boundary layer grows with decreasing Re and in all cases the velocity decreases monotonically towards the wall.

In order to get an estimate about the extension of the thermal boundary as a function of the heated length z/d the Fig. 4(b) shows an isoplot of the temperature rise ΔT along the rod. The isoplot is generated at the same inlet conditions and composed of the time averaged values of the TC-rake at several positions z/d (in 532 total averaged TC signals).

As one can easily see from Fig. 4(b), the thermal boundary layer establishes already upstream the heated surface. One reason for the upstream heating is that the Biot number Bi, accounting for the heat resistance of the fluid compared to that through which the heat flux is passing through is not infinite, it amounts to $Bi = 12.38$. Thus, an upstream distance over about two characteristic length of the rod is calculated, which is also found in the experiment. As the flow proceeds from $z/d = 0$ to larger values in axial direction the thermal boundary layer increases monotonically up to the position $z/d = 13.57$. Then the convective radial turbulent heat flux caused by the radial momentum transport is dominating the energy transfer. This is reflected by an almost constant thermal boundary layer thickness. The reason for the non-symmetry of the temperatures of the upper and lower half is the non-concentricity mentioned before. As the fluid passes $z/d = 24$ the thermal boundary continuously decreases. A part of this decrease can be explained by the same effect, which caused the upstream heating of the fluid, namely that part of the supplied heat flux is not normally entering the fluid

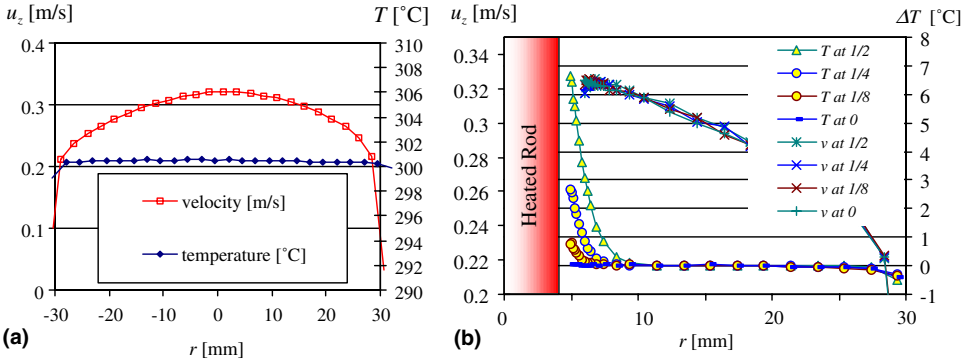

Fig. 3. (a) Measured u_z and temperature distribution at $T = 300$ °C, $Re = 10^5$; (b) measured mean u_z and temperature rise ΔT (°C) as a function of r, z/d at $T_{in} = 300$ °C, $Re = 10^5$.

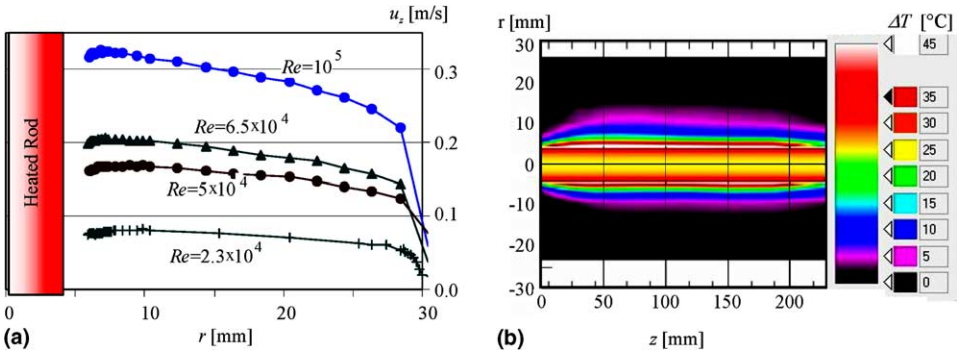

Fig. 4. (a) Measured mean velocity u_z (m/s) as a function of r (mm) at T_{in} = 300 °C for different Re at z/d = 13.9; (b) isoplot of the temperature rise ΔT as a function of r and z/d for T_{in} = 300 °C and $Re = 10^5$.

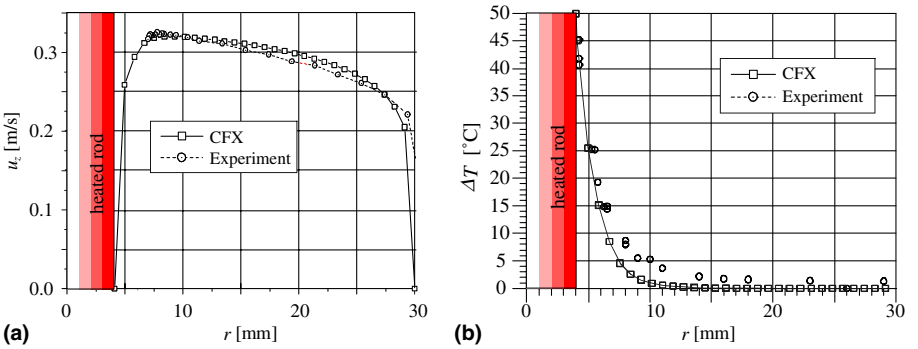

Fig. 5. Comparison between measured and calculated mean velocity (a) and temperature rise (b) as a function of r for T_{in} = 300 °C, $Re = 10^5$ ($Pe = 2.2 \times 10^4$), $q'' = 34.051$ W/cm^2 at z/d = 14.02.

domain. It rather flows in the steel housing of the rod and enters the fluid after the heated length leading there to a temperature rise.

In Fig. 5(a) and (b) the mean velocity and radial temperature rise ΔT distribution are depicted at the position z/d = 14.02 as a function of r. They are compared to the CFX simulation results.

The comparison of the velocities exhibits a nearly perfect agreement between the simulation and the experimental values. The maximum deviations in the main flow field amount maximum to ±5%. Numerical parametric studies show that these deviations in the flow field can be already caused by experimental imperfections in the range of 0.1 mm (!), which could appear just by the differential elongations caused by the heater in the experiment. The finite spatial extension of the Pitot tube leads also to a radial integration of the velocity signal close to the wall, where the largest gradients appear. Considering both effects the deviations found shrink down to ±3%.

Regarding the radial temperature distribution the deviations between experiment and model are significantly larger as Fig. 5(b) illustrates. The computed fluid–wall interface temperature is for all z/d positions larger than measured. At the position z/d = 14.02 the measured value is about 11.7% lower (50.3 °C calculated versus 45 °C measured) than the predicted one. Taking into that the thermocouple integrates the measured value over its radial extension of 0.25 mm the deviations are minimized to 3.1 °C, which is about +7%.

Although the fluid–wall interface temperature is captured with a sensible resolution by the computation the qualitative shape of the thermal boundary layer is not resolved by the simulation. The radial extension of the calculated thermal boundary layer is significantly smaller than the experimental one. Since the temperature gradient towards the wall ($\partial T/\partial r = 0$) is close to zero for both, heat losses towards the environment do not contribute to this deviation. In order to overcome these deviations in the simulation turbulent heat flux models has to be embedded in the turbulence model for low Prandtl number fluid.

5. Conclusions and outlook

The heated rod experiment investigates the turbulent heat transfer of a heavy liquid metal flow along a heated

cylinder within an annular duct at surface heat fluxes of $q'' \geqslant 30$ W/cm^2. The use of miniaturized Pitot tubes acting as velocity sensors in turbulent HLM flows was demonstrated successfully. The measured velocity distributions coincide with the numerically predicted values. The fluid–wall interface temperatures measured agree within 7% with the numerically predicted ones in the parameter range investigated here. Although the last named issue is the most important one from an engineering point of view since it describes the heat transfer capability of a flow configuration in terms of local Nusselt numbers, larger deviations exist regarding the spatial extension of the thermal boundary layer. They can not only be explained by the imperfections of the experimental set-up. Parts of these deviations originate from the improper description of the turbulent radial heat fluxes within the turbulence models while using them in low Prandtl number fluids. This effect is more significant if additionally buoyancy effects occur. Therefore, it is planned to run the heated rod experiment at lower Reynolds numbers and higher surface heat fluxes, in order to set-up a data basis for the development of more sophisticated models.

Acknowledgments

This work is supported by the HGF Strategy Fund Project under the Förderkennzeichen 01SF9926/ and the European ASCHLIM project (ASsessments of CFD-Codes for Heavy LIquid Metals) with the EU-contract number FIKW-CT2001-80121.

References

[1] L.N. Carteciano, Entwicklung eines Turbulenzmodells für Auftriebsströmungen, Dissertation, FZKA-Report 5775, 1996.
[2] L.N. Carteciano, M. Wörner, G. Grötzbach, Erweiterte Turbulenzmodelle für technische Anwendungen von FLUTAN auf Naturkonvektion, Jahrestagung Kerntechnik, INFORUM Bonn 1999, S129.
[3] L. Barleon, U. Burr, M. Frank, R. Stieglitz, K.-J. Mack, MHD flow and heat transfer in a rectangular duct, FZKA-Report 5927, 1998.
[4] U. Burr, L. Barleon, U. Müller, A. Tsinober, J. Fluid Mech. 406 (2000) S247.
[5] ASCHLIM 2002, Assessment for computational codes in heavy liquid metal flows, EU-Contract number FIKW-CT2001-80121.
[6] W. Vieser, Th. Esch, F. Menter, CFX-5 Solver Theory, CFX, United Kingdom, 2002.
[7] V. Imbeni, C. Martini, S. Masini, G. Palombarini, The properties of the eutectic alloys Pb55.5Bi and Pb17Li, ENEA-Report DT-EUB-00001, Part 2, 1999.
[8] H. Schlichting, Grenzschichttheorie, Verlag G. Braun Karlsruhe, 1982.
[9] E. Truckenbrodt, Fluidmechanik I, II, Springer, Berlin/Heidelberg/New York, 1980.